Table 5. Statistical Analysis No. 2

	Multivariate Logistic Regression (R^2 = 0.17, n = 46)		
	P	Odds Ratio	95% CI
Duration: 2 times*	0.004	1.81	1.20–2.97
Preoperative tibialis anterior: 2–3– and 0–1	0.049	0.29	0.08–1.00
Gender: male-female	0.091	3.12	0.83–12.67
Age: 10 yr	0.289	1.25	0.83–1.93

*Preoperative duration of palsy.
CI indicates confidence interval.

■ Discussion

In spinal anatomy, the L4 and L5 nerve roots are distributed throughout the tibialis anterior,[11,12] and it is mainly the L4 nerve root that controls tibialis anterior movement. So, impairment of the L4 nerve root was thought to commonly cause drop foot. But in this study, the main lesion occurred in the L4/5 segment, with only 3 patients presenting with a L3/4 single lesion, and there was no extraforaminal lesion in the L4/5 segment. None of these 3 patients with L3/4 single lesion complained of radicular symptoms. In addition, if tibialis anterior would be ruled by L4 nerve root, there would be cases with drop foot due to L4 radiculopathy, but, actually, we have never experienced drop foot with L4 radiculopathy so far. From the results of the current study, we could conclude that drop foot would be mainly caused by an impairment of the L5 nerve root and that this root mainly rules the tibialis anterior.

In an investigation of cases with drop foot caused by degenerative lumbar diseases, Girardi *et al*[13] reported that no statistically significant relationship was found between the extent of recovery and age, diagnosis (herniated nucleus pulposus or lumbar spinal stenosis), duration of symptoms, or severity of preoperative weakness. In their investigation, however, the authors defined drop foot as a muscle weakness of the tibialis anterior, scoring less than 4 out of 5. The weakest tibialis anterior strength observed in a patient was 2 out of 5, while no patients presented with a preoperative tibialis anterior strength of 0–1. In our clinical experiences, patients with tibialis anterior strength of 4 out of 5 do not show drop foot at all. By contrast, we defined drop foot as a muscle weakness of the tibialis anterior scoring less than 3 out of 5, in compliance with the Medical Research Council guidelines. Moreover, 17 patients (37%) in our study presented with a preoperative tibialis anterior strength of 0–1. Focusing exclusively on those patients with a preoperative tibialis anterior strength of 2–3–, we demonstrate recovery from drop foot in 76% (22/29, 14 excellent and 8 good cases) of cases.

In a previous study on recovery from motor deficits, there are some reports concerning postoperative motor deficits as neurologic complications,[7–9] however, there are few reports concerning preoperative motor deficits. Postacchini *et al*[14] reported an inverse relationship between the severity of the preoperative motor deficit and ability to recover complete motor function in contrast to the findings of Girardi *et al*.[13] In the current study, we have found improved surgical outcome in the patients with shorter duration of palsy and higher strength of tibialis anterior, which supports the results of Postacchini *et al*,[14] and all patients who had completely recovered had palsy for 3 months or less, but there was a patient who had a 4-day duration of drop foot who did not recover at all.

Concerning the recovery process, Jonsson and Stromqvist[15] reported that most recovery occurred during the first 4 months following surgery. In the current study, we describe 14 patients who made a full recovery. Of these, the shortest duration to reach full tibialis anterior strength was 6 weeks, while the longest duration was 2 years (Figure 3). Taking these results into consideration, progress of recovery could be prospected 2 years after surgery.

A clinical question that might arise is whether to operate on a patient suffering from drop foot but without any leg pain. In the current study, 8 patients presented in this manner, 5 of which (63%) made a full recovery. There was no significant difference in neurologic recovery (P = 1.000) between these patients and those suffering from leg pain, suggesting that drop foot without radicular pain due to degenerative lumbar diseases can be treated effectively with surgery.

In the current study, age at surgery significantly affected postoperative tibialis anterior strength, and the risk increased by 1.45 times with each 10-year rise in age, as shown by a Mann-Whitney *U* test. However, the multiple regression analysis failed to show a relationship between age at surgery and postoperative tibialis anterior strength. We speculate that the significant Mann-Whitney *U* test resulted from the tendency for older age patients to have suffered a longer duration of symptoms.

■ Conclusion

Severity of palsy before surgery and duration of symptoms are considered to be key prognostic factors for successful surgery for drop foot, while compression pathology (herniated or canal stenosis), age at surgery, neurologic involvement, leg pain, and number of compressed segments have little effect on surgical outcome.

■ Key Points

- Of patients, 61% recovered from drop foot after surgery.
- Preoperative strength of the tibialis anterior and duration of palsy were factors that most affected the surgical outcome.
- Cases with painless palsy can be successfully treated with operation.

References

1. Baysefer A, Erdogan E, Sali A, et al. Foot drop following brain tumors: Case reports. *Minim Invasive Neurosurg* 1998;4:97–8.
2. Hassan FO, Shannak A. Primary pelvic hydatid cyst: An unusual cause of sciatica and foot drop. *Spine* 2001;26:230–2.
3. Reynolds F. Damage to the conus medullaris following spinal anaesthesia. *Anaesthesia* 2001;56:238–47.
4. Ahmad FU, Pandey P, Sharma BS, et al. Foot drop after spinal anesthesia in a patient with a low-lying cord. *Int J Obstet Anesth* 2006;15:233–6.
5. Miller DB Jr. Arthroscopic meniscus repair. *Am J Sports Med* 1988;16:315–20.
6. Jurist KA, Greene PW III, Shirkhoda A. Peroneal nerve dysfunction as a complication of lateral meniscus repair: A case report and anatomic dissection. *Arthroscopy* 1989;5:141–7.
7. Epstein NE. Nerve root complications of percutaneous laser-assisted diskectomy performed at outside institutions: A technical note. *J Spinal Disord* 1994;7:510–2.
8. Carreon LY, Puno RM, Dimar JR II, et al. Perioperative complications of posterior lumbar decompression and arthrodesis in older adults. *J Bone Joint Surg Am* 2003;85:2089–92.
9. Okuda S, Miyauchi S, Oda T, et al. Surgical complications of posterior lumbar interbody fusion with total facetectomy in 251 patients. *J Neurosurg Spine* 2006;4:304–9.
10. Campbell WW. *The Neurologic Examination*. Philadelphia, PA: Lippincott Williams & Wilkins; 2005.
11. Hoppenfeld S, Hutton R. *Physical Examination of the Spine and Extremities*. New York, NY: Appleton-Century Crofts; 1976.
12. Frymoyer JW, Wiesel SW. *The Adult and Pediatric Spine*. 3rd ed. Philadelphia, PA: Lippincott Williams & Wilkins; 2004.
13. Girardi FP, Cammisa FP Jr, Huang RC, et al. Improvement of preoperative foot drop after lumbar surgery. *J Spinal Disord Tech* 2002;15:490–4.
14. Postacchini F, Giannicola G, Cinotti G. Recovery of motor deficits after microdiscectomy for lumbar disc herniation. *J Bone Joint Surg Br* 2002;84:1040–5.
15. Jonsson B, Stromqvist B. Motor affliction of the L5 nerve root in lumbar nerve compression syndromes. *Spine* 1995;20:2012–15.

Available online at www.sciencedirect.com
ScienceDirect
Biochemical and Biophysical Research Communications 354 (2007) 453–458
BBRC
www.elsevier.com/locate/ybbrc

Bone marrow-derived osteoblast progenitor cells in circulating blood contribute to ectopic bone formation in mice

Satoru Otsuru [a,b], Katsuto Tamai [a,*], Takehiko Yamazaki [a], Hideki Yoshikawa [b], Yasufumi Kaneda [a]

[a] *Division of Gene Therapy Science, Osaka University Graduate School of Medicine, 2-2 Yamada-oka, Suita, Osaka 565-0871, Japan*
[b] *Department of Orthopaedic Surgery, Osaka University Graduate School of Medicine, 2-2 Yamada-oka, Suita, Osaka 565-0871, Japan*

Received 18 December 2006
Available online 10 January 2007

Abstract

Recent studies have suggested the existence of osteoblastic cells in the circulation, but the origin and role of these cells *in vivo* are not clear. Here, we examined how these cells contribute to osteogenesis in a bone morphogenetic protein (BMP)-induced model of ectopic bone formation. Following lethal dose-irradiation and subsequent green fluorescent protein-transgenic bone marrow cell-transplantation (GFP-BMT) in mice, a BMP-2-containing collagen pellet was implanted into muscle. Three weeks later, a significant number of GFP-positive osteoblastic cells were present in the newly generated ectopic bone. Moreover, peripheral blood mononuclear cells (PBMNCs) from the BMP-2-implanted mouse were then shown to include osteoblast progenitor cells (OPCs) in culture. Passive transfer of the PBMNCs isolated from the BMP-2-implanted GFP-mouse to the BMP-2-implanted nude mouse led to GFP-positive osteoblast accumulation in the ectopic bone. These data provide new insight into the mechanism of ectopic bone formation involving bone marrow-derived OPCs in circulating blood.

Keywords: Bone morphogenetic protein; Ectopic bone; Circulating osteoblast progenitor cells; Bone marrow transplantation

BMP-2 and other members of the BMP family are well-known inducers of bone formation *in vitro* and *in vivo* [1]. During healing of bone fractures, stimulation from BMPs recruits OPCs to the fracture sites and induces their differentiation to become osteoblasts. An experimental model of ectopic bone formation in mice has also indicated that BMP-2 stimulation is essential for the recruitment of OPCs to the osteogenic sites [2]. The source and the route for the recruitment of the OPCs in this model, however, have not been fully elucidated. Notably, the surrounding soft tissues, the periosteum and the bone marrow all constitute potential origins for the OPCs involved in osteogenesis, but it is unclear how these OPCs target the region expressing BMPs [3].

Recent studies have shown the existence of OPCs (or indeed osteoblasts) in the circulating blood of various mammals, including humans [4–6]. These reports indicate an ability of circulating cells to function as osteoblasts in culture and to form osseous tissues after transplantation, suggesting that OPCs and/or osteoblasts may be supplied via the circulation to regenerating bone *in vivo*. This hypothesis is potentially an attractive one for the field of bone-regenerative medicine, especially if an adequate number of circulating OPCs can be isolated from peripheral blood, expanded in culture, and delivered to sites requiring bone regeneration. However, the origins of circulating OPCs and evidence of endogenously circulating cells with the potential to migrate and contribute to bone regeneration *in vivo* have not yet been fully demonstrated.

Abbreviations: OPCs, osteoblast progenitor cells; BMPs, bone morphogenetic proteins; MOPCs, marrow-derived OPCs; GFP, green fluorescent protein; BMT, bone marrow transplantation; PBMNCs, peripheral blood mononuclear cells; DAPI, 6-diamidino-2-phenylindole; FITC, fluorescein isothiocyanate; H&E, hematoxylin and eosin; TRAP, tartrate-resistant acid phosphatise.

* Corresponding author. Fax: +81 6 6879 3909.
E-mail address: tamai@gts.med.osaka-u.ac.jp (K. Tamai).

0006-291X/$ - see front matter © 2007 Elsevier Inc. All rights reserved.
doi:10.1016/j.bbrc.2006.12.226

Here, we report for the first time that marrow-derived OPCs (MOPCs) can migrate to a BMP-2 pellet implanted into mouse muscle and differentiate to become osteoblasts within the BMP-2-induced ectopic bone. We have also succeeded in culturing circulating OPCs from PBMNCs isolated from BMP-2-implanted mice. Furthermore, intravenous transfer of the GFP-transgenic PBMNCs containing OPCs to nude mice implanted with BMP-2 pellet generates a significant number of GFP-osteoblasts in the BMP-2-induced ectopic bone. We believe that these new findings will accelerate further understanding of the role of circulating OPCs, not only in ectopic osteogenesis, but also in the healing of bone fractures *in vivo*.

Materials and methods

Bone marrow cell transplantation (BMT). Under sterile conditions, bone marrow cells were isolated from 8- to 10-week-old male C57BL/6 transgenic mice that ubiquitously expressed enhanced GFP [7]. Eight- to 10-week-old female C57BL/6 mice were lethally irradiated with 10 Gy. For BMT, each irradiated mouse received 5×10^6 bone marrow cells from GFP transgenic mice. Experiments on BMT mice were performed at least 6 weeks after BMT. All animals were handled according to approved protocols and the guidelines of the Animal Committee of Osaka University.

Preparation and implantation of BMP-2-containing collagen pellets. Recombinant human BMP-2 was provided by Astellas Pharma Inc. (Tokyo, Japan). The BMP-2 was suspended in buffer solution (5 mmol/L glutamic acid, 2.5% glycine, 0.5% sucrose, and 0.01% Tween 80) at a concentration of 1 μg/μL. Next, 3 μL (3 μg of BMP-2) of the BMP-2 solution was diluted in 22 μL PBS and blotted onto a porous collagen disc (6 mm diameter, 1 mm thickness), freeze-dried, and stored at −20 °C. All procedures were carried out under sterile conditions. BMP-2-containing or control PBS-containing collagen pellets were implanted onto the backs (below muscle fascia) of BMT mice, C57BL/6 mice, or nude mice. Three weeks later, fluorescent photos of ectopic bone formation were taken using a digital microscope (Multiviewer system VB-S20 KEYENCE, Osaka, Japan).

Morphological and immunofluorescent analysis of the ectopic bone. Ectopic bone was removed and fixed with 4% paraformaldehyde at 4 °C for 48 h. After taking soft X-ray photos, the bones were decalcified at 4 °C for 6 days with the EDTA solution replaced every other day. After decalcification, the pellets were equilibrated in PBS containing 15% sucrose for 12 h and then in PBS containing 30% sucrose for 12 h, embedded in Tissue-Tec OCT Compound (Sakura Finetek Japan, Tokyo, Japan), and frozen on dry ice and stored at −20 °C. For immunofluorescence staining, 6-μm-thick sections were cut with a Cryostat (Leica Microsystems AG, Wetzlar, Germany). After washing, the sections were treated with 0.1% trypsin (Difco Laboratories, Detroit, MI) in PBS for 30 min at 37 °C to activate antigens. Then the sections were blocked with normal goat serum for 1 h before incubation with polyclonal anti-mouse osteocalcin antibody (1:250, Takara Bio Inc., Shiga, Japan). Subsequently, sections were stained with Alexa Fluor 546 goat anti-rabbit secondary antibody (Molecular Probes, Eugene, OR) for 2 h. Then, sections were stained with 4′,6-diamidino-2-phenylindole (DAPI) for 10 min at room temperature and mounted with anti-fade solution VECTOR Shield (Vector Laboratories, Inc., Burlingame, CA).

GFP and tartrate-resistant acid phosphatase (TRAP) double staining of the ectopic bone. For GFP immunohistochemistry, 6-μm-thick sections of BMP-2-induced ectopic bone were treated with 0.6% hydrogen peroxide in 80% methanol for 30 min and then 3% hydrogen peroxide in PBS for 15 min to inhibit endogenous peroxidase. Then the sections were blocked with normal goat serum for 1 h before incubation with polyclonal anti-GFP antibody (1:250, MBL, Nagoya, Japan). Signals were detected using diaminobenzidine. Subsequently, to detect osteoclasts, TRAP staining was carried out using a staining kit (Cell Garage, Tokyo, Japan) according to the manufacturer's protocol. Counterstaining was performed with hematoxylin.

Culture of MOPCs in PBMNCs. Peripheral blood was taken from the heart of BMP-2-implanted mice with a 24-gauge needle and 1-ml syringe containing heparin and enriched for light-density mononuclear cells (PBMNCs) by Ficoll-Paque (Amersham Biosciences AB, Uppsala, Sweden) centrifugation. Red blood cells were removed by resuspending in 0.125% Tris–NH_4Cl buffer and sieving through a nylon mesh. To culture MOPCs, were then inoculated in basal medium consisting of DMEM supplemented with 10% FCS, 100 U/mL streptomycin/penicillin, and 50% conditioned culture medium (DMEM with 10% FCS) of mouse bone marrow-mesenchymal cells as a growth factor supplement (Otsuru and Tamai, unpublished data). To induce osteoblast differentiation, those cells were cultured in the osteogenic medium consisting of IMDM supplemented with 0.1 μM dexamethasone (Nacalai Tesque, Kyoto, Japan), 10 mM β-glycerol phosphate (Sigma, Saint Louis, MO), and 0.05 mM ascorbic acid 2-phosphate (Sigma) for 3–4 weeks. Cells were then fixed with 4% paraformaldehyde for 10 min and treated with 0.2% Triton X in phosphate-buffered saline (PBS) for 10 min.

Immunostaining of cultured MOPCs. Cultured MOPCs were pretreated with 3% skim milk (Nacalai Tesque) in PBS for 1 h before incubation with polyclonal anti-mouse osteocalcin antibody (1:250, Takara Bio Inc.), monoclonal anti-mouse alkaline phosphatase antibody (1:250, R&D Systems, Minneapolis, MN) or polyclonal anti-mouse osteopontin antibody (1:250, LSL, Tokyo, Japan). Subsequently, sections were stained with Alexa Fluor 546 goat anti-rabbit or anti-rat IgG secondary antibody (Molecular Probes) for 2 h. Those cells were stained with 4′,6-diamidino-2-phenylindole (DAPI) for 10 min at room temperature and mounted with the anti-fade solution VECTOR Shield (Vector Laboratories, Inc.).

Passive transfer of PBMNCs from BMP-2-implanted GFP-mouse to BMP-2-implanted nude mouse. For passive transfer of PBMNCs containing MOPCs, nude mice implanted with BMP-2-containing collagen pellets were injected with PBMNCs from the GFP-transgenic BMP-2-implanted mice via a tail vein. Injections were carried out everyday for one week.

Results

Bone marrow-derived cells contribute to BMP-2-induced ectopic bone formation

We first evaluated whether bone marrow-derived cells are involved in the process of BMP-2-induced ectopic bone formation. We implanted BMP-2 pellets under the muscular fascia in the backs of GFP-BMT mice that had been transplanted with GFP-transgenic bone marrow cells after lethal dose irradiation (Fig. 1A). Three weeks after the implantation of BMP-2 collagen pellets, intense GFP fluorescence had accumulated in the region of the BMP-2-induced ectopic bone (Fig. 1B). Immunohistological analysis revealed that a significant number of GFP-positive cells expressing osteocalcin (OC) were seen lining the newly generated bone (Fig. 1C). Tartrate-resistant acid phosphatase (TRAP) and GFP double staining revealed that some of the GFP-positive lining cells were TRAP-positive osteoclasts, which were clearly distinguishable from GFP-positive/TRAP-negative positive cells (Fig. 1D).

Successful culture of OPCs in PBMNCs from a BMP-2-implanted mouse

To determine if a BMP-2-implanted mouse contained OPCs in circulating blood, we isolated PBMNCs from a BMP-2-implanted mouse and cultured those cells in the con-

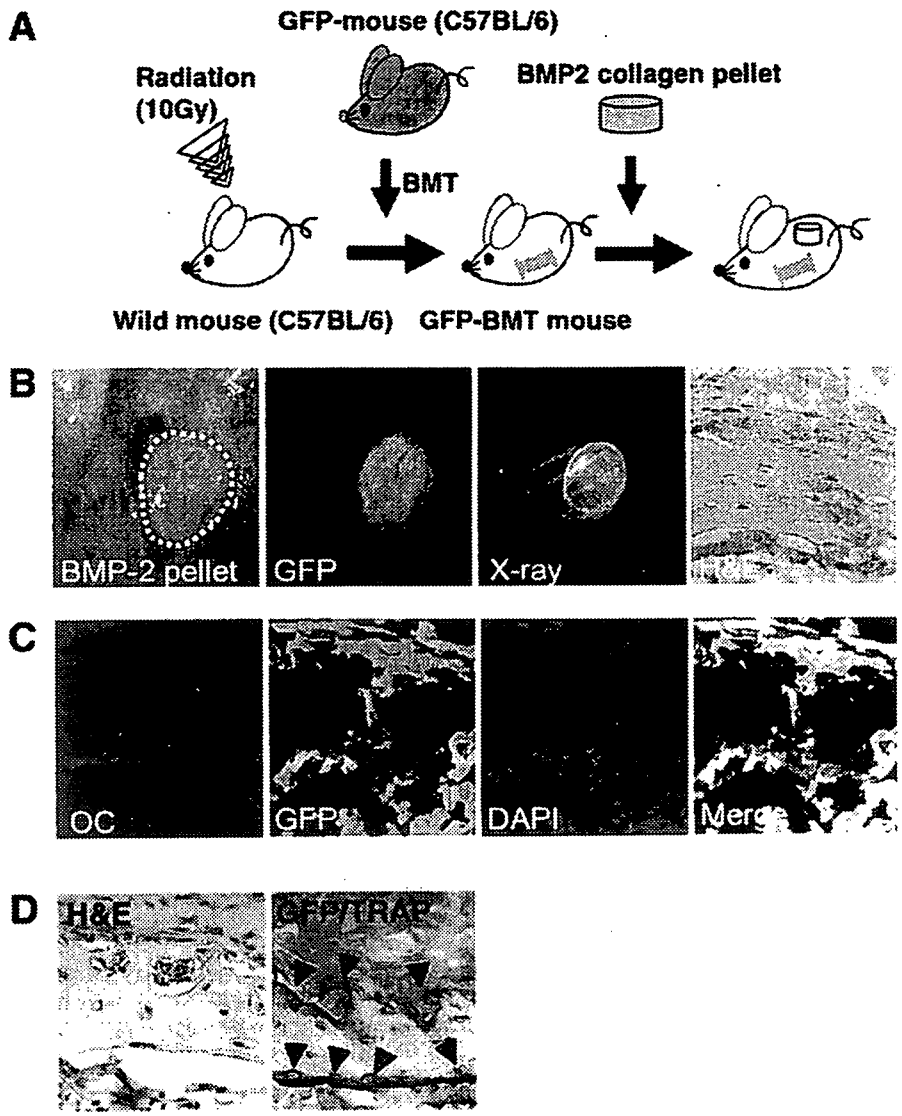

Fig. 1. Bone marrow-derived osteoblast progenitor cells contribute to BMP-2-induced ectopic bone formation in GFP-BMT mice. (A) A BMP-2 pellet is shown implanted under the muscular fascia of a GFP-BMT mouse. (B) A BMP-2 pellet shows accumulation of GFP fluorescence three weeks after implantation. Soft X-ray photo of the BMP-2 pellet demonstrates that ectopic bone has formed in the BMP-2 pellet. Histologic section stained with hematoxylin and eosin (H&E) of the BMP-2 pellet also reveals bone formation in the BMP-2 pellet. Magnification, 400×. (C) Immunofluorescence staining shows that cells lining the newly generated ectopic bone are osteoblasts expressing osteocalcin (OC), and that some of those cells show GFP fluorescence (GFP), revealed as yellow-colored cells in merged picture (Merge) of OC, GFP and DAPI staining (DAPI). Magnification, 400×. (D) GFP and TRAP double staining reveals that the bone marrow-derived osteoclasts (red arrow-head) as well as bone marrow-derived non-osteoclastic cells (brown arrow-head) line the newly formed ectopic bone. Magnification, 400×.

ditioned culture medium, as described in the methods section (Fig. 2A). As we expected, adhesive stromal type cells successfully expanded in culture. Then we looked at the expression of osteoblast-specific proteins before and after induction of osteogenic differentiation. OP, a marker of undifferentiated osteoblasts, was shown to be expressed in the cultures without induction of differentiation (Fig. 2B). Under these culture conditions, however, the differentiation-specific makers ALP and OC were not expressed (Fig. 2B). After change of culture medium to the osteogenic medium, however, these cells then expressed and secreted abundant ALP and OC as well as OP in the culture medium (Fig. 2C).

Intravenous transplantation of GFP-PBMNCs provides GFP-osteoblasts in the ectopic bone in the BMP-2-implanted nude mouse

To confirm further that significant numbers of MOPCs mobilize from bone marrow to peripheral blood and contribute to ectopic bone formation, we isolated PBMNCs

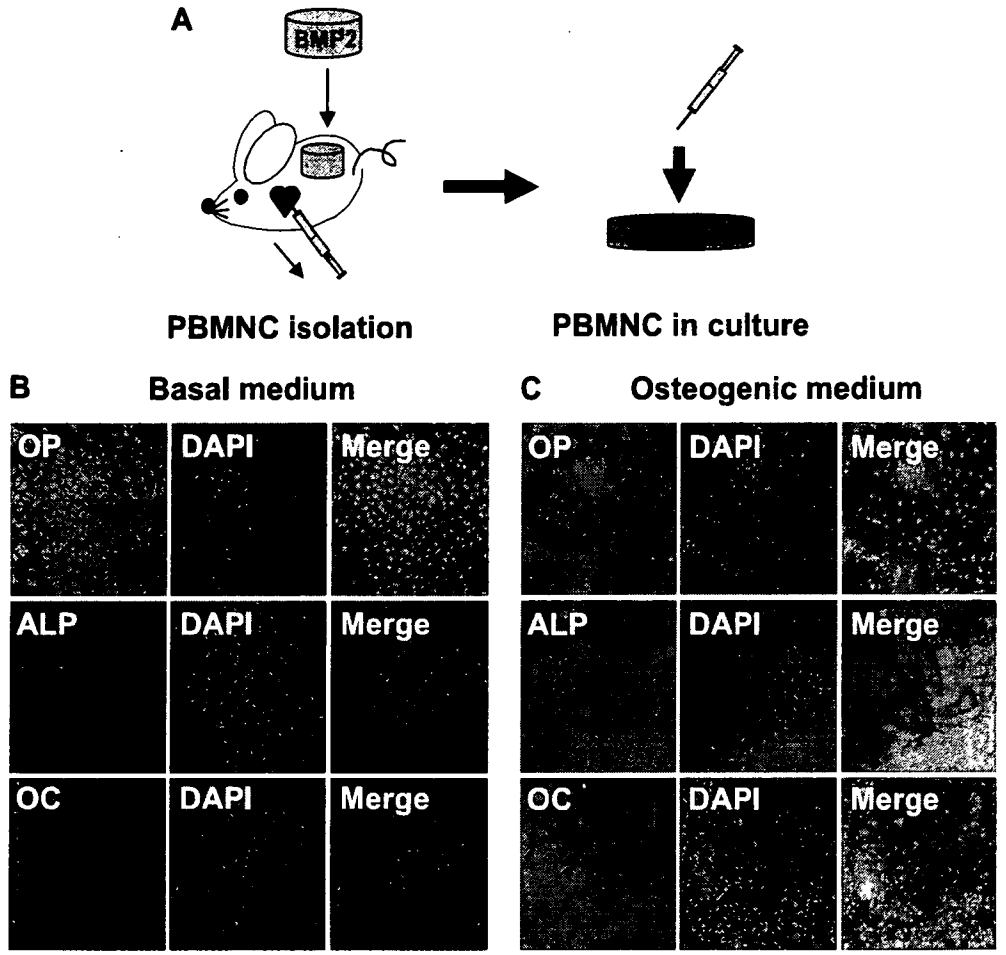

Fig. 2. OPCs in PBMNCs from a BMP-2-implanted mouse express bone matrix proteins in culture. (A) Cultured PBMNCs isolated from peripheral blood of a BMP-2-implanted mouse. (B) Immunofluorescence staining of the cultured cells from isolated PBMNCs shows only osteopontin (OP) expression in normal medium. (C) When those cells were cultured in osteogenic medium, however, there is positive immunoreactivity for alkaline phosphatase (ALP) and osteocalcin (OC) as well as OP. The staining patterns and DAPI staining (DAPI) are shown in the merged image (Merge). Magnification, 200×.

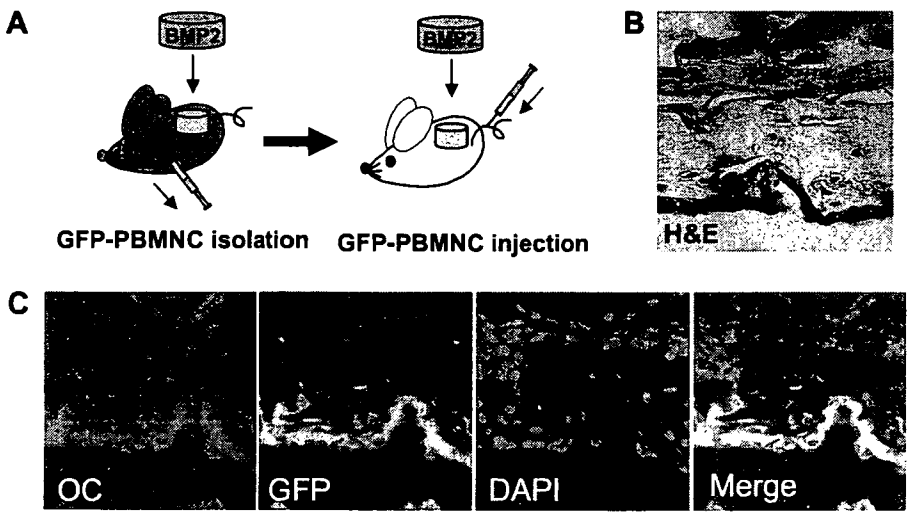

Fig. 3. OPCs in PBMNCs can contribute to ectopic bone formation in a BMP-2 pellet. (A) A nude mouse implanted with a BMP-2 pellet is injected daily for 7 days with PBMNCs taken from BMP-2-implanted GFP transgenic mice. (B) A histologic H&E-stained section shows ectopic bone formation in the BMP-2 pellet. Magnification, 400×. (C) Immunofluorescence staining of the newly generated ectopic bone shows that osteocalcin-expressing osteoblasts (OC) and GFP-positive cells derived from the injected PBMNCs (GFP) co-localize with yellow-colored cells in the merged picture (Merge) with DAPI staining (DAPI). Magnification, 400×.

everyday from BMP-2 pellet-implanted GFP-transgenic mice and injected the isolated PBMNCs (1×10^6) through the tail veins of BMP-2 pellet-implanted nude mice daily for 7 days (Fig. 3A). Two weeks later, the implanted pellets were recovered and examined histologically. We observed that GFP-positive osteoblasts originating from the injected PBMNCs contributed significantly to ectopic bone formation in the mice (Fig. 3B).

Discussion

Circulating mesenchymal precursor/stem cells or osteoblast lineage cells have been shown to exist in various mammals, including humans and mice [4–6,8,9]. Moreover, those circulating mesenchymal/osteoblast lineage cells have been isolated from peripheral blood, expanded in culture, and inoculated to show their potency to become osteoblasts both *in vitro* and *in vivo*. Nevertheless, a number of important questions have been raised following those observations, including as to where those circulating cells came from and where they went *in vivo*? In this study, we have shown, for the first time, clear evidence that marrow cells in intact bone are the major, if not the exclusive, source of circulating OPCs in an *in vivo* model of ectopic bone formation using BMP-2-stimulation in mouse muscle. Of note, our GFP-BMT mouse model showed that ~40% of osteocalcin-producing cells in the ectopic bone were derived from MOPCs, suggesting that endogenous circulating MOPCs may contribute to ectopic bone formation observed in various pathological conditions, and possibly, to fracture healing. Other findings that showed the need for adequate blood flow to obtain mature bone regeneration also add credence to the importance of MOPCs in the circulation [10].

Currently, little is known about the signals that trigger the migration of OPCs from the bone marrow into the circulation and this was not addressed in detail in the current study. Vascular endothelial growth factor (VEGF) previously has been shown to have the capacity to recruit marrow-derived vascular endothelial progenitor cells [11] and we also observed elevation of VEGF levels in the muscle around the implanted BMP-2 pellets (data not shown). This observation may suggest that VEGF contributes to angiogenesis in the area of bone regeneration, although further evidence is needed to support this hypothesis.

The importance of providing additional OPCs to sites of new bone formation has been shown in a number of previous studies [12–17]. From a clinical perspective, identification of signals that induce migration of MOPCs into the circulation could have potential future clinical applications, since increasing MOPCs in the circulation may help patients with delayed or non-union of bone fractures by increasing the number of MOPCs at the bone repair site. The ability to induce circulating MOPCs to enter the peripheral blood circulation may also enable us to easily isolate these cells by simple venous blood sampling, thus providing an opportunity to develop novel cell-based regenerative therapies for bone fractures and possibly for other damaged tissues. Because current procedures to isolate mesenchymal cells directly from the bone marrow are invasive and carry a possible risk of bone marrow infection, the easier approach of isolating MOPCs from peripheral blood has advantages in terms of safety, repeatability, and acceptability. In addition, this method may also be helpful in developing new therapies for genetic disorders such as osteogenesis imperfecta through genetic manipulation of isolated MOPCs [18,19]. Thus, further investigation of circulating MOPCs is warranted to more precisely characterize their cell biology and the mechanisms that lead to their induction. Such work may have very exciting implications for novel therapeutic strategies in bone regenerative medicine.

Acknowledgments

This work was partially supported by Funds of the Ministry of Education, Culture, Sports, Science and Technology, and Grant-in-Aids from the Ministry of Public Health and Welfare. We would like to thank Professor John A McGrath for his technical support.

References

[1] J.M. Wozney, V. Rosen, A.J. Celeste, L.M. Mitsock, M.J. Whitters, R.W. Kriz, R.M. Hewick, E.A. Wang, Novel regulators of bone formation: molecular clones and activities, Science 242 (1988) 1528–1534.

[2] K. Takaoka, H. Nakahara, H. Yoshikawa, K. Masuhara, T. Tsuda, K. Ono, Ectopic bone induction on and in porous hydroxyapatite combined with collagen and bone morphogenetic protein, Clin. Orthop. Relat. Res. (1988) 250–254.

[3] L.C. Gerstenfeld, D.M. Cullinane, G.L. Barnes, D.T. Graves, T.A. Einhorn, Fracture healing as a post-natal developmental process: molecular, spatial, and temporal aspects of its regulation, J. Cell. Biochem. 88 (2003) 873–884.

[4] G.Z. Eghbali-Fatourechi, J. Lamsam, D. Fraser, D. Nagel, B.L. Riggs, S. Khosla, Circulating osteoblast-lineage cells in humans, N. Engl. J. Med. 352 (2005) 1959–1966.

[5] S.A. Kuznetsov, M.H. Mankani, S. Gronthos, K. Satomura, P. Bianco, P.G. Robey, Circulating skeletal stem cells, J. Cell. Biol. 153 (2001) 1133–1140.

[6] C. Wan, Q. He, G. Li, Allogenic peripheral blood derived mesenchymal stem cells (MSCs) enhance bone regeneration in rabbit ulna critical-sized bone defect model, J. Orthop. Res. 24 (2006) 610–618.

[7] M. Okabe, M. Ikawa, K. Kominami, T. Nakanishi, Y. Nishimune, Green mice as a source of ubiquitous green cells, FEBS Lett. 407 (1997) 313–319.

[8] M. Fernandez, V. Simon, G. Herrera, C. Cao, H. Del Favero, J.J. Minguell, Detection of stromal cells in peripheral blood progenitor cell collections from breast cancer patients, Bone Marrow Transplant. 20 (1997) 265–271.

[9] C.A. Roufosse, N.C. Direkze, W.R. Otto, N.A. Wright, Circulating mesenchymal stem cells, Int. J. Biochem. Cell Biol. 36 (2004) 585–597.

[10] J. Glowacki, Angiogenesis in fracture repair, Clin. Orthop. Relat. Res. (1998) S82–S89.

[11] M. Grunewald, I. Avraham, Y. Dor, E. Bachar-Lustig, A. Itin, S. Yung, S. Chimenti, L. Landsman, R. Abramovitch, E. Keshet, VEGF-induced adult neovascularization: recruitment, retention, and role of accessory cells, Cell 124 (2006) 175–189.

[12] L.J. Curylo, B. Johnstone, C.A. Petersilge, J.A. Janicki, J.U. Yoo, Augmentation of spinal arthrodesis with autologous bone marrow in a rabbit posterolateral spine fusion model, Spine 24 (1999) 434–438, discussion 438–439.

[13] R.E. Grundel, M.W. Chapman, T. Yee, D.C. Moore, Autogeneic bone marrow and porous biphasic calcium phosphate ceramic for segmental bone defects in the canine ulna, Clin. Orthop. Relat. Res. (1991) 244–258.

[14] T.S. Lindholm, O.S. Nilsson, T.C. Lindholm, Extraskeletal and intraskeletal new bone formation induced by demineralized bone matrix combined with bone marrow cells, Clin. Orthop. Relat. Res. (1982) 251–255.

[15] T.S. Lindholm, P. Ragni, T.C. Lindholm, Response of bone marrow stroma cells to demineralized cortical bone matrix in experimental spinal fusion in rabbits, Clin. Orthop. Relat. Res. (1988) 296–302.

[16] K. Takagi, M.R. Urist, The role of bone marrow in bone morphogenetic protein-induced repair of femoral massive diaphyseal defects, Clin. Orthop. Relat. Res. (1982) 224–231.

[17] J.R. Werntz, J.M. Lane, A.H. Burstein, R. Justin, R. Klein, E. Tomin, Qualitative and quantitative analysis of orthotopic bone regeneration by marrow, J. Orthop. Res. 14 (1996) 85–93.

[18] J.R. Chamberlain, U. Schwarze, P.R. Wang, R.K. Hirata, K.D. Hankenson, J.M. Pace, R.A. Underwood, K.M. Song, M. Sussman, P.H. Byers, D.W. Russell, Gene targeting in stem cells from individuals with osteogenesis imperfecta, Science 303 (2004) 1198–1201.

[19] E.M. Horwitz, D.J. Prockop, L.A. Fitzpatrick, W.W. Koo, P.L. Gordon, M. Neel, M. Sussman, P. Orchard, J.C. Marx, R.E. Pyeritz, M.K. Brenner, Transplantability and therapeutic effects of bone marrow-derived mesenchymal cells in children with osteogenesis imperfecta, Nat. Med. 5 (1999) 309–313.

Sagittal Alignment of the Subaxial Cervical Spine After C1-C2 Transarticular Screw Fixation in Rheumatoid Arthritis

Yoshihiro Mukai, MD, PhD, Noboru Hosono, MD, PhD,† Hironobu Sakaura, MD,‡ Ryutaro Fujii, MD,‡ Motoki Iwasaki, MD, PhD,‡ Tsuyoshi Fuchiya, MD,§ Keiju Fujiwara, MD, PhD,§ Takeshi Fuji, MD, PhD,† and Hideki Yoshikawa, MD, PhD‡*

Abstract: Several articles reported the association between the development of subaxial kyphosis and the hyperlordotic fixation of C1-C2. However, their patients were heterogeneous in both primary disease and operative procedure. Transarticular screw fixation has become a popular procedure for C1-C2 arthrodesis instead of wiring techniques in which C1-C2 is difficult to fix in the intended alignment. Furthermore, in rheumatoid arthritis (RA) patients, subaxial lesions play an important role in potential subaxial alignment changes. The subaxial influences after C1-C2 transarticular screw fixation in patients with RA are unclear. To investigate the radiographic features of the subaxial cervical spine after C1-C2 transarticular screw fixation for RA, we reviewed 28 cases of C1-C2 transarticular screw fixation for rheumatoid atlanto-axial subluxation. The sagittal alignment of C1-C2 and the subaxial cervical spine was measured and the factors that affect subaxial alignment were investigated. Subaxial alignment became less lordotic in the postoperative course. The C1-C2 fixation angle and subaxial alignment showed a negative linear correlation. However, no significant correlation was found between changes in the C1-C2 angle and changes in the subaxial alignment. Four patients had a postoperative kyphotic subaxial deformity. Neurologic deterioration recurred in 4 patients, because of the postoperative development of subaxial subluxation. Common radiographic changes included an increase in C1-C2 lordosis, constant inclination of C1, an anterior shift of C2, and a decrease in C2-C7 lordosis. Many factors, not only C1-C2 angle, are associated with subaxial sagittal alignment change after C1-C2 transarticular screw fixation.

Received for publication May 30, 2006; accepted December 3, 2006.

From the *Department of Orthopedic Surgery, Sumitomo Hospital; ‡Department of Orthopedic Surgery, Osaka University Graduate School of Medicine; †Department of Orthopedic Surgery, Osaka Koseinenkin Hospital; and §Department of Orthopedic Surgery, Osaka Prefectural General Medical Center, Osaka, Japan.

No funds were received in support of this work.

No benefits in any form have been or will be received from a commercial party related directly or indirectly to the subject of this manuscript.

The manuscript submitted does not contain information about medical device(s)/drug(s).

Reprints: Yoshihiro Mukai, MD, PhD, Department of Orthopedic Surgery, Sumitomo Hospital, 5-3-20 Nakanoshima, Kita-ku, Osaka, 530-0005, Japan (e-mail: mukai-y@umin.ac.jp).

Key Words: rheumatoid arthritis, C1/C2, atlanto-axial subluxation, fusion, Magerl procedure, subaxial alignment, subaxial subluxation

(*J Spinal Disord Tech* 2007;20:436–441)

The upper cervical spine is well known to be affected by various kinds of pathologies and often must be fused surgically to relieve the cord compression and/or intractable pain. Despite excellent results of C1-C2 posterior arthrodesis, several authors[1,2] have reported postoperative malalignment of the subaxial cervical spine after the procedure. Yoshimoto et al[2] reported that 42% of the patients who underwent C1-C2 arthrodesis showed the progression of kyphosis in the subaxial cervical spine, and that C1-C2 fixation in a hyperlordotic position led to subaxial kyphosis after the surgery. This conclusion, however, is of limited significance, because these previous studies involved a variety of surgeries and diseases including rheumatoid arthritis (RA). Posterior wiring techniques were formerly the standard procedures to fuse C1-C2.[3–6] Tightening of a wire passed around the laminae of C1 and C2 tended to approximate these laminae and often impose a hyperlordosis. Recently, however, transarticular screw fixation has become a popular procedure for C1-C2 arthrodesis in place of wiring techniques.[7,8] C1-C2 can be aligned more freely by this procedure than by wiring techniques. In patients with RA, subaxial cervical alignment is affected not only by C1-C2 fusion but also by subaxial lesions including subaxial subluxation (SAS), commonly recognized and often progressive among patients with RA. There has been no detailed study of subaxial changes after C1-C2 transarticular screw fixation in patients with RA. We retrospectively investigated subaxial changes after C1-C2 transarticular screw fixation exclusively in patients with RA.

MATERIALS AND METHODS

Between 1995 and 2001, 35 patients with rheumatoid atlanto-axial subluxation underwent C1-C2 transarticular screw fixation supplemented with posterior wiring or lamina clamping. Patients who underwent concomitant surgery on the subaxial region were excluded from the study. Two patients died within 2 years after the

surgery: one from myocardial infarction and the other from brain infarction. Five patients were lost to the minimum 2-year follow-up; thus, the remaining 28 patients (4 men and 24 women) provided the data in this study. A monocortical autograft from the iliac crest was used in each patient. The mean age of patients at surgery was 60.2 years (range, 34 to 74 y) and the mean follow-up period was 6.0 years (range, 2 to 10 y) after the surgery. All patients fulfilled the American Rheumatism Association criteria for RA. The indication for surgery was intolerable neck pain and/or cervical myelopathy caused by C1-C2 subluxation. Blinded measurement of sagittal spinal curve was conducted by one of the authors (Y.M.), who was not directly involved in the surgeries nor in the follow-up of patients using a modified Harrison posterior tangent method.[9] Radiographs, taken with the patient in the upright or sitting position, were scanned using a high quality image scanner and the digital data were transmitted to a computer work station, where measurement was performed using a software program (PopImaging Version 3.5; Digital Being Kids, Kanagawa, Japan). The bony landmarks to be identified on lateral neutral radiographs were all postero-superior and postero-inferior vertebral body corners of C2-C7, the mid-C1 anterior arch, and the mid-C1 posterior arch. Relative rotational angle (RRA_{Cm-Cn}) is the segmental angle derived from posterior vertebral tangents passing through the 2 points of the posterior vertebral body corners of Cm and Cn (Fig. 1). RRA_{C1-C2} was obtained from the angle between the posterior vertebral tangent of C2 and the perpendicular to the line through the centers of the anterior and posterior arches of C1 (Fig. 1). RRA was defined to have a negative (−) value in segmental lordosis and a positive (+) value in segmental kyphosis. The absolute rotation angle (ARA_{C2-C7}) was defined as the summation of the angles from RRA_{C2-C3} to RRA_{C6-C7}. The atlas plane angle (APA) was the angle derived from the horizontal line and the line passing through the centers of the anterior and posterior arches of C1 (Fig. 2). Negative (−) APA meant C1 in an extension position with respect to the horizontal plane. The horizontal translation of C2 from C7, which was defined as the distance from the postero-superior body corner of C2 to a vertical line through the postero-inferior body corner of C7, was termed Tz_{C2-C7} (Fig. 2). The RRA from C1-C2 to C6-C7, the ARA_{C2-C7}, the APA, and the Tz_{C2-C7} were measured on lateral neutral radiographs before surgery, 1 month after surgery, 1 year after surgery, and at the final follow-up. Subaxial vertebral slippage (≥ 3 mm) was regarded as significant SAS if accompanied by rheumatoid lesions such as erosive changes in facet joints, intervertebral discs, endplates, or spinous processes.

Neurologic impairment was evaluated using the Ranawat classification (class I, no neural deficit; class II, subjective weakness with hyperreflexia and dysesthesia; class IIIA, objective weakness and long tract signs but ambulating; and class IIIB, objective weakness and long tract signs and not ambulating).[10] Neck pain was also classified using Ranawat grading (0, none; 1, mild; 2, moderate; and 3, severe).[10] Clinical assessment was conducted just before the surgery, 1 year after the surgery, and at the final follow-up. The relationship between clinical status and the change in subaxial cervical alignment was also investigated.

Paired *t* test, Student *t* test, analysis of variance, and correlation coefficient methods were used for statistical analysis. Probability values less than 0.05 were considered statistically significant. Analyses were performed using JMP statistical computer software, version 5.0 (SAS Institute, Cary, NC).

RESULTS

Radiographic Evaluation

C1 Inclination

The mean APA before surgery was −11.2 ± 12.0 degrees; 1 month after surgery, it was −15.9 ± 8.8 degrees; 1 year after surgery, it was −12.9 ± 8.5 degrees; and at the final follow-up, it was −12.0 ± 9.2 degrees. The C1 inclination came into a more extended position with respect to the horizontal line just after the surgery and it returned to its preoperative inclination subsequently. However, there was no statistical difference among these values.

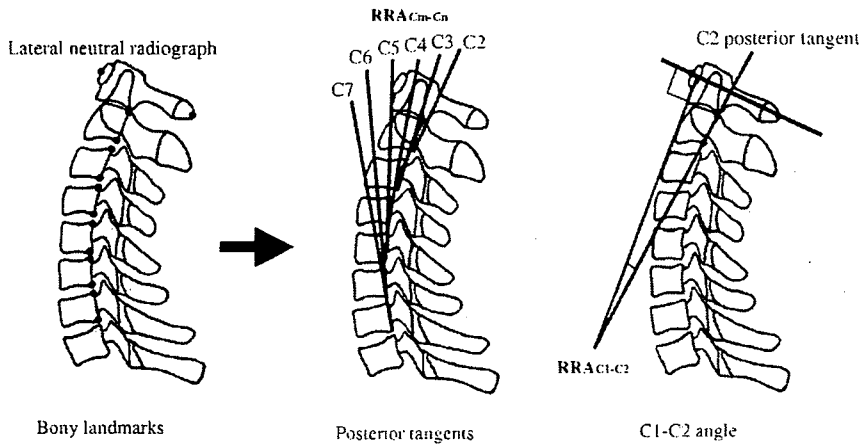

FIGURE 1. Relative rotational angle (RRA_{Cm-Cn}).

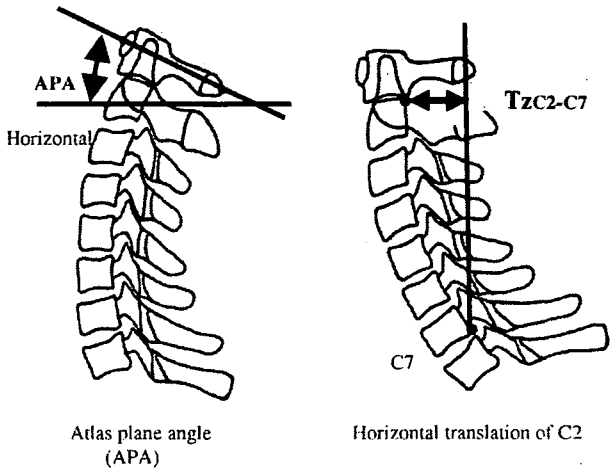

FIGURE 2. Atlas plane angle (APA) and horizontal translation ($Tz_{C2\text{-}C7}$).

C1-C2 Alignment

The mean $RRA_{C1\text{-}C2}$ before surgery was -6.0 ± 11.9 degrees; 1 month after surgery, it was -13.1 ± 9.8 degrees; 1 year after surgery, it was -12.7 ± 9.5 degrees; and at the final follow-up, it was -13.5 ± 9.4 degrees. The lordosis in C1-C2 was significantly increased by surgery (-6.0 vs. -13.1 degrees, $P = 0.0016$) and showed no significant change in the postoperative course. There was a positive linear correlation between preoperative and postoperative $RRA_{C1\text{-}C2}$ ($R = 0.535$, $P = 0.0028$) (Fig. 3A); the more lordotic the preoperative C1-C2 alignment was, the more lordotic the C1-C2 fixation angle became.

Horizontal Translation of C2

The mean horizontal translation ($Tz_{C2\text{-}C7}$) before surgery was 3.3 ± 13.0 mm; 1 month after surgery, it was 8.4 ± 12.4 mm; 1 year after surgery, it was 9.7 ± 12.4 mm; and at the final follow-up, it was 12.9 ± 15.0 mm. C2 progressively shifted forward with respect to C7 postoperatively ($P = 0.0030$).

Subaxial Alignment

No patients had SAS and only 1 patient had a positive value of $ARA_{C2\text{-}C7}$ on a lateral neutral radiograph preoperatively. The mean $ARA_{C2\text{-}C7}$ before surgery was -20.2 ± 13.2 degrees; 1 month after surgery, it was -19.5 ± 13.6 degrees; 1 year after surgery, it was -15.5 ± 13.0 degrees; and at the final follow-up, it was -13.3 ± 15.6 degrees. The subaxial cervical spine became less lordotic with increasing postoperative time ($P = 0.0293$). The $RRA_{C1\text{-}C2}$ one month after surgery, which was also the C1-C2 fixation angle, and the $ARA_{C2\text{-}C7}$ one year after surgery showed a negative linear correlation ($R = -0.516$, $P = 0.0043$) (Fig. 3B); the more lordotic the alignment in which C1-C2 was fixed by surgery, the less lordotic the subaxial alignment became postoperatively. However, no significant correlation was found between the operative changes of $RRA_{C1\text{-}C2}$ and the postoperative changes of $ARA_{C2\text{-}C7}$ 1 year after surgery ($R = -0.180$, $P = 0.362$) (Fig. 4A) or at the final follow-up ($R = 0.070$, $P = 0.731$) (Fig. 4B) (Fig. 5). Postoperative positive conversion of $ARA_{C2\text{-}C7}$, which indicates the development of subaxial kyphosis, was found in 4 patients (14%) during the follow-up. In 3 of them, the kyphosis was closely related to the deterioration of preoperative rheumatoid subaxial lesions, such as erosive changes of the facet or endplate. Postoperative development of SAS was noted in 5 patients (18%), all of whom had some degree of preoperative subaxial lesions preceding subluxation (Fig. 6). No statistical association was found between postoperative $RRA_{C1\text{-}C2}$ and the postoperative development of SAS.

Clinical Evaluation

Preoperatively, 25 patients (89%) had neck pain; all of them indicated pain relief by 1 or 2 grades of Ranawat category 1 year after the surgery. During the follow-up period, neck pain deteriorated in 5 patients; in 2 of these patients, the development of subaxial kyphosis was noted.

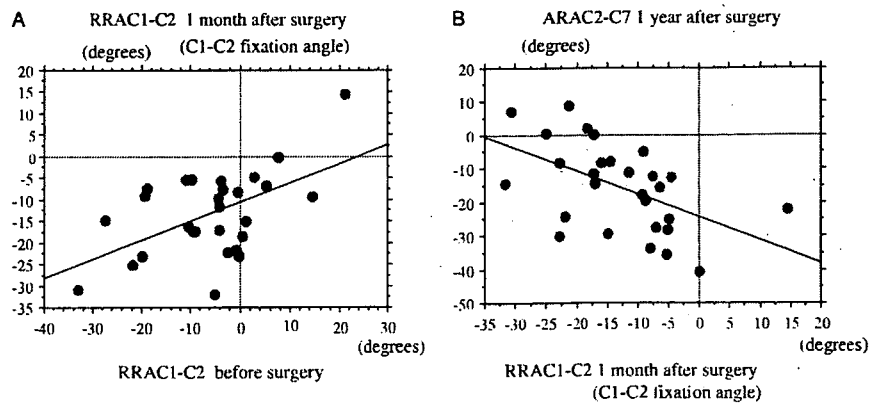

FIGURE 3. A, Correlation between preoperative and postoperative C1-C2 angles ($R = 0.535$, $P < 0.01$). B, Correlation between C1-C2 fixation angle and subaxial alignment 1 year after surgery ($R = -0.516$, $P < 0.01$).

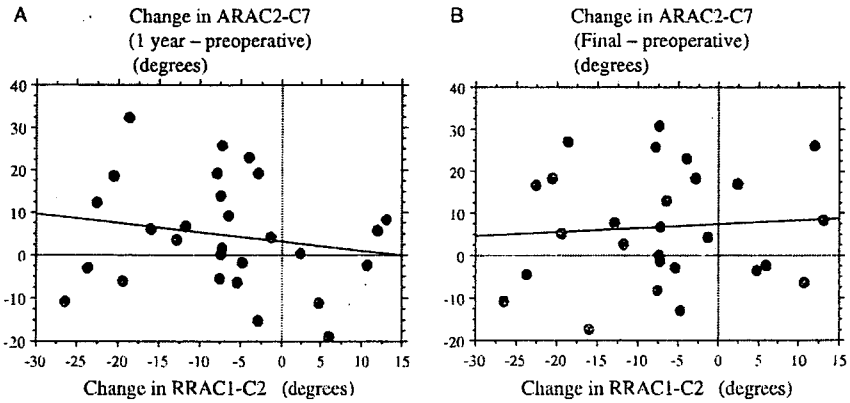

FIGURE 4. A, Correlation between the operative changes of C1-C2 alignment and the changes of subaxial alignment before surgery and 1 year after surgery ($R = -0.180$, $P = 0.362$). B, Correlation between the operative changes of C1-C2 alignment and the changes of subaxial alignment before surgery and at the final follow-up ($R = 0.070$, $P = 0.731$).

Preoperative neurologic status was class I in 5 patients, class II in 14 patients, class IIIA in 5 patients, and class IIIB in 4 patients. Of the 9 patients with neurologic status in class IIIA or class IIIB, 7 showed postoperative improvement by one or more grades of Ranawat class, although the remaining 2 with class IIIB status had no neurologic improvement. Neurologic status deteriorated in 4 patients during the postoperative follow-up, because of the development of SAS. Postoperative alignment change did not result in neurologic worsening by itself, unless SAS was also present.

DISCUSSION

RA commonly involves the cervical spine with potential risks for pain or progressive myelopathy in patients with long-standing RA. Disorders related to RA occur predominantly in the upper cervical region, where surgical treatments have been extensively documented.[11–13] C1-C2 arthrodesis has been traditionally performed using posterior wiring techniques, which may have some difficulties with nonunion or loss of correction between C1 and C2.[3–6] Recent articles[14] report high fusion rates with few complications associated with transarticular screw fixation procedure introduced by Magerl and Seemann.[7] However, we often encounter a subaxial alignment change, which can be a cause of neurologic impairment after C1-C2 arthrodesis. Previous studies on subaxial changes after C1-C2 fusion are of little use in predicting those changes for patients with RA, because those studies enrolled patients with various etiologies of C1-C2 instability. Subaxial lesions can develop not only as a natural course of RA[15–17] but also as a consequence of upper cervical fusion or disruption of the extensor muscles involved in posterior cervical surgery. For these reasons, we chose to focus our study

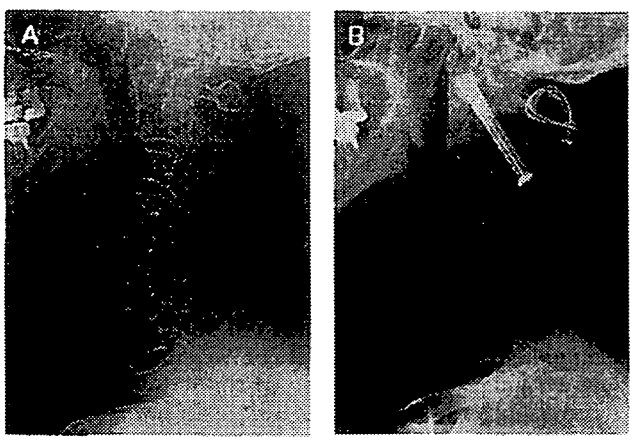

FIGURE 5. A, Preoperative lateral neutral radiograph of 52-year-old woman. B, C1-C2 angle decreased by 7 degrees postoperatively. Ten years after surgery, there was only 7-degree increase in $ARA_{C2\text{-}C7}$.

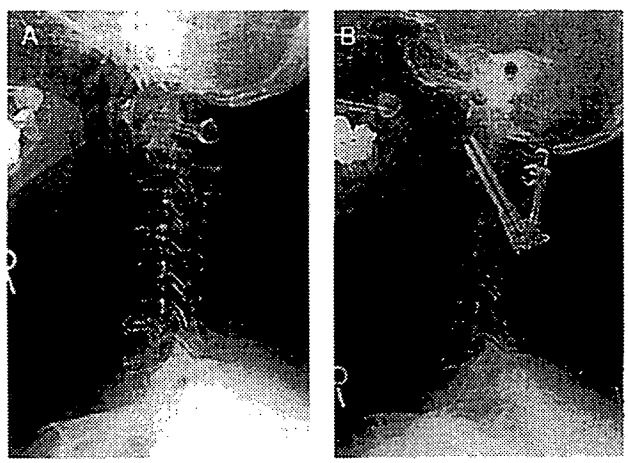

FIGURE 6. A, Preoperative lateral neutral radiograph of 56-year-old woman. Slight subluxation and facet erosion were found at C4-C5. B, C1-C2 angle decreased by 7 degrees postoperatively. Four years after surgery, marked subluxation and angular deformity were developed at C4-C5.

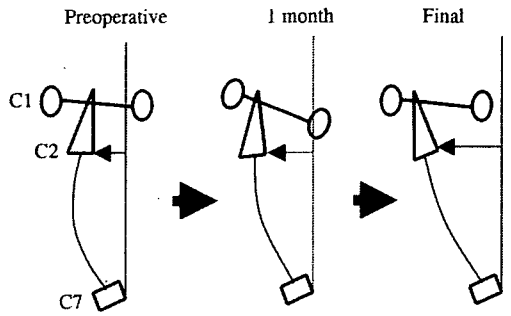

FIGURE 7. Radiographic features after C1-C2 transarticular screw fixation in patients with RA were an increase in C1-C2 lordosis, an anterior shift of C2, a decrease in C2-C7 lordosis, and the tendency of C1 inclination to return to preoperative inclination.

on C1-C2 transarticular screw fixation for rheumatoid atlanto-axial subluxation. There has been no detailed study of the subaxial changes after C1-C2 transarticular screw fixation in patients with RA.

From our study, the radiographic changes after C1-C2 transarticular screw fixation in patients with RA are summarized as follows: (1) an increase in C1-C2 lordosis, (2) a progressive ventral shift of C2 relative to C7, (3) a progressive decrease in C2-C7 lordosis, and (4) a tendency of C1 inclination to return to preoperative inclination (Fig. 7). When radiographs are taken with patients in a neutral position, patients are asked to face straight ahead. Preoperative alignment of the skull-C1 complex in a neutral position may be a natural alignment for individual patient. The postoperative increase of C1-C2 lordosis, which caused an increase in C1 inclination, may have been compensated by a decrease in subaxial cervical lordosis so as to return the C1 inclination to the preoperative one. Actually, in our study, there was a negative linear correlation between the postoperative alignments of C1-C2 and C2-C7, which is consistent with the previous report[2] (Fig. 3B). On the other hand, no significant correlation was found between the operative changes of $RRA_{C1\text{-}C2}$ and the postoperative changes of $ARA_{C2\text{-}C7}$ (Figs. 4A, B). This is opposite to the conventional idea that the more the lordosis in C1-C2 increases from surgery, the more the subaxial kyphosis that develops. The postoperative increase in C1 inclination owing to an increase in C1-C2 lordosis may be counterbalanced by not only the subaxial cervical alignment but also by the thoracolumbar spine alignment to keep the C1 inclination constant, but current study has no data about that.

Postoperative kyphosis in the subaxial cervical spine, which was noted in 4 of the 28 patients (14%), did not develop as often as previously considered and was closely associated with the deterioration of preexisting subaxial lesions. The mean C1-C2 fixation angle of these patients was −20.5 degrees (range, −17 to 25 degrees), which was not excessively lordotic. Although the C1-C2 fixation angle was less lordotic than the preoperative one in 7 patients (25%), 2 of them had a concomitant decrease in subaxial lordosis. In these patients, factors other than the C1-C2 fixation angle might play an important role in subaxial alignment. Previous studies[18,19] have reported that cervical alignment after posterior surgery is significantly affected by detachment of the semispinalis muscles from the spinous process of the axis. Because of the ligament weakness inherent to RA, muscle dissection can also accelerate subaxial lesions and may lead to subaxial kyphosis.

In this study, development of instability at C2-C3, which was adjacent to the fused segment, was not found. The greatest postoperative kyphosis or SAS developed at C4-C5 or C3-C4, accompanied by the deterioration of subaxial lesions.

So far, only the C1-C2 fixation angle has been emphasized as a key to regulate postoperative subaxial alignment in C1-C2 arthrodesis. In patients with RA, however, subaxial alignment is regulated by multiple factors: the C1-C2 angle, the development and/or progression of subaxial lesions, and the disruption of extensor muscles. These factors are difficult to evaluate correctly and subaxial change after C1-C2 arthrodesis for RA is hard to predict. Although we could not demonstrate the optimal C1-C2 fixation angle from this study, we do not necessarily deny the argument that C1-C2 fixation in excessive lordotic or kyphotic alignment should be avoided to prevent subaxial malalignment after the surgery. Regarding neurologic status, alignment change without SAS did not by itself cause neurologic worsening, whereas compression myelopathy caused by SAS was the main cause for postoperative neurologic deterioration.

REFERENCES

1. Toyama Y, Koyanagi T. The optimum position of fusion in atlanto-axial arthrodesis. *Seikei Geka (Japanese)*. 1994;45:495–502.
2. Yoshimoto H, Itoh M, Abumi K, et al. A retrospective radiographic analysis of subaxial sagittal alignment after posterior C1-C2 fusion. *Spine*. 2004;29:175–181.
3. Gallie WE. Fractures and dislocations of the cervical spine. *Am J Surg*. 1939;46:495–499.
4. McGraw R, Rusch RM. Atlanto-axial arthrodesis. *J Bone Joint Surg Br*. 1973;55:482–489.
5. Brooks A, Jenkins E. Atlanto-axial arthrodesis by the wedge compression method. *J Bone Joint Surg Am*. 1978;60:279–284.
6. Dickman C, Sonntag V, Paradopoulos S, et al. The interspinous method of posterior atlantoaxial arthrodesis. *J Neurosurg*. 1991; 74:190–198.
7. Magerl F, Seemann PS. Stable posterior fusion of the atlas and axis by transarticular screw fixation. In: Kerl P, Weidner A, eds. *Cervical Spine I*. Vienna: Springer-Verlag; 1987:322–327.
8. Grob D, Jeanneret B, Aebi M, et al. Atlantoaxial fusion with transarticular screw fixaion. *J Bone Joint Surg Br*. 1991;73: 972–976.
9. Harrison DE, Harrison DD, Cailliet R, et al. Cobb method or Harrison posterior tangent method: which to choose for lateral cervical radiographic analysis. *Spine*. 2000;25:2072–2078.

10. Ranawat CS, O'Leary P, Pellici P, et al. Cervical spine fusion in rheumatoid arthritis. *J Bone Joint Surg Am.* 1979;61: 1003–1010.
11. Boden SD, Dodge LD, Bohlman HH, et al. Rheumatoid arthritis of the cervical spine. A long-term analysis with predictors of paralysis and recovery. *J Bone Joint Surg Am.* 1993; 75:1282–1297.
12. Cabot A, Becker A. The cervical spine in rheumatoid arthritis. *Clin Orthop.* 1978;131:130–140.
13. Lipson SJ. Rheumatoid arthritis in the cervical spine. *Clin Orthop.* 1989;239:121–127.
14. Gluf WM, Schmidt MH, Apfelbaum RI. Atlantoaxial transarticular screw fixation: a review of surgical indications, fusion rate, complications, and lessons learned in 191 adult patients. *J Neurosurg Spine.* 2005;2:155–163.
15. Winfield J, Cooke D, Brook AS, et al. A prospective study of the radiological changes in the cervical spine in early rheumatoid disease. *Ann Rheum Dis.* 1981;40:109–114.
16. Yonezawa T, Tsuji H, Matsui H, et al. Subaxial lesions in rheumatoid arthritis. Radiographic factors suggestive of lower cervical myelopathy. *Spine.* 1995;20:208–215.
17. Fujiwara K, Owaki H, Fujimoto M, et al. A long term follow-up study of cervical lesions in rheumatoid arthritis. *J Spinal Disord.* 2000;13:519–526.
18. Nolan JP, Sherk HH. Biomechanical evaluation of the extensor musculature of the cervical spine. *Spine.* 1988;13:9–11.
19. Iizuka H, Shimizu T, Tateno K, et al. Extensor musculature of the cervical spine after laminoplasty: morphologic evaluation by coronal view of the magnetic resonance image. *Spine.* 2001;26: 2220–2226.

● 多因子病のゲノム研究は今

多因子病の遺伝的要因をどのように考えるべきか

東海大学医学部 教授

井ノ上 逸朗 Ituro Inoue

要 旨

この1年で多くの疾患で大規模なゲノム全域アソシエーション・スタディがなされ，革新的な成果が上がっている．糖尿病，心筋梗塞などの多因子疾患の感受性遺伝子が続々と報告され，追試までなされている．わずかな違いながら確実な感受性遺伝子同定ができている．その経緯を述べるとともに，今後の展開について考えてみたい．

はじめに

生命現象は複雑系である．ゲノムサイエンス以前の時代には，この複雑系を生物学的手法で包括的に理解することは不可能であった．同様に，複雑な要因が関与する多因子疾患を古典的遺伝学で理解することは困難である．ゲノムサイエンスによりシステム生物学が登場し，複雑系の包括的理解が試みられるようになった．また，多因子疾患へのアプローチ法も変革してきた．多因子疾患の遺伝要因をどのように同定するか，この10年来，遺伝学者の議論の中心にあった．30年前，2型糖尿病を遺伝学者の悪夢と称したJames Neelを引用するまでもなく，多因子疾患の遺伝要因へのアプローチは混沌としたものであっ

キーワード：ゲノム全域アソシエーション・スタディ，多因子疾患，疾患遺伝子研究

た．ところが，ヒトゲノム配列決定，一塩基多型（SNP）データベースの拡充，国際 HapMap 計画の完了といった流れの中で，ゲノム全域を網羅する SNP タイピングプラットフォームが開発され，一気に事情が変わってきた．ゲノム全域を密に網羅する 30～50 万 SNP でのアソシエーション・スタディにより，続々と疾患感受性遺伝子多型が同定されており，同時に追試もなされ再現性が確認されている．感受性遺伝子が同定されると，疾患発症への機能的関与，他の遺伝要因，かつ環境要因との相互作用も検証がなされるであろう．今，疾患遺伝子研究は時代のうねりの中にある．もう大波はきている．大波に押しつぶされるか，波にうまく乗れるか，どっちだろうか．

多因子疾患の遺伝要因を同定する困難さ

まず多因子疾患の遺伝解析における古典的な問題点を挙げよう．

① 遺伝的浸透率が低い
② メンデルの遺伝法則に従わない
③ 世代を隔てた家系収集が困難
④ 表現模写の存在（遺伝要因が存在しないのに発症）
⑤ 遺伝的異質性の存在（ローカス，アレル）
⑥ 遺伝子間，遺伝子–環境要因間相互作用の存在

多因子疾患では一つひとつの遺伝要因の効果は小さいと考えられる．1つの遺伝子変異により発症する単一遺伝病との大きな違いである．当然，遺伝的に浸透率は小さくなり，そのためメンデルの遺伝法則には従わない．また，関与する遺伝要因の検出も困難となる．家系収集し連鎖解析で遺伝子座を特定する手法は，単一遺伝病では効果的であった．しかしながら，多因子疾患では上記のようメンデル遺伝に従わないことに加え，高齢発症が多いため多世代の家系が困難であること，家系内非罹患者でも未発症の可能性がある，などの理由でモデルを設定しない罹患同胞対連鎖解析が行われる（図1）．この手法では組換え情報が入らないため，遺伝子座のピンポイントができず，連鎖領域は通常 20 cM に及ぶことが多い．また，通常遺伝子座は複数特定される．そうするとゲノムの1％以上の領域をアソシエーション・スタディにより徹底的に調べ抜く必要が生じる．そんなことなら

図1 多因子疾患のゲノム解析

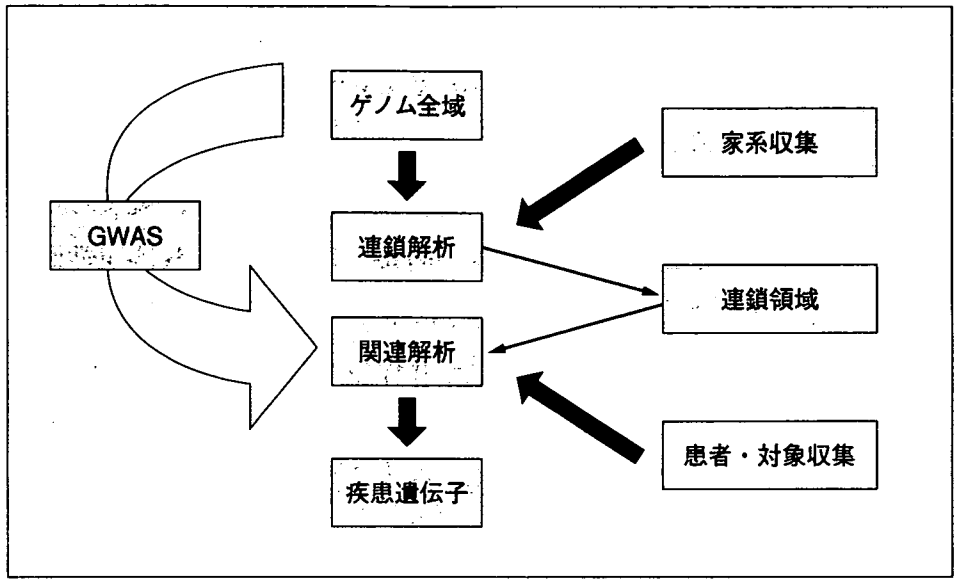

GWAS：ゲノム全域アソシエーション・スタディ

始めからゲノム全域でアソシエーション・スタディを試みる手法が効果的と議論されてきた．図1に示すよう連鎖解析，アソシエーション・スタディと順を追うより，初めからゲノム全域アソシエーション・スタディ（GWAS）を行った方が効率的となってきているかも知れない．

ゲノム全域アソシエーション・スタディ（GWAS）

すでに10年前にRischとMerikangasにより，遺伝的効果の弱い因子の検出にはアソシエーション・スタディの方が有利なことが示されていた[1]．ただ，それは未知の感受性遺伝子にヒットしたと想定しての統計遺伝学的検討であった．当時，連鎖解析のための遺伝マーカー（マイクロサテライト）は解析に十分な間隔で装備されていたので，家系数さえ十分ならゲノム全域解析で遺伝子座を特定できる確率は高かった．しかしながら，アソシエーション・スタディのための遺伝マーカー（SNP）は密に存在しておらず，また網羅的なタイピング法も開発されていなかった．この2年で様相は一変し，GWASが盛んに行われるようになった．Affymetrix，Illumina両社により，続々とスケールアップされる形でタイピングプラットフォームが開発されている．Affymetrixは906,600のSNP，946,000コピー数変異検出のた

めのプローブが配置されたGenome－wide SNP Array 6.0®を出している．一方，Illuminaには550,000 SNPをタイピングできるHuman-Hap550 Genotyping BeadChip®がある．

この1年で“Nature”，“Nature Genetics”，“Science”誌に論文掲載されたGWASの例を示す（表1）．一目瞭然であるが，膨大な数の成果が出てきている．それぞれが大規模スタディであり，注目すべきは糖尿病における TCF7L2 のように異なるスタディで再現性が得られていることである．その中でも最も大規模なアソシエーション・スタディの結果を紹介する．Wellcome Trust Case Conrol Consortium において7疾患について2,000例ずつの患者群と3,000例の対照でのアソシエーション・スタディが報告されている[2]．対象となった疾患は躁うつ病，冠動脈疾患，クローン病，関節リウマチ，1型糖尿病，2型糖尿病そして高血圧である．タイピングプラットフォームはAffymetrix GeneChip 500K Mapping Array Set®が採用されている．統計解析はArmitage trend testを用いており，$5X10^{-7}$以下を強いシグナルとしている．躁うつ病で1個，冠動脈疾患で1個，クローン病で9個，関節リウマチで3個，1型糖尿病で7個，2型糖尿病で3個の SNP が同定された．高血圧では強いシグナルを得ることはできなかった．既報の結果を再現した SNP も多く，間違いのない遺伝要因を検出できていると考えていいだろう．

すべての遺伝要因を現在のプラットフォームで検出できるか．答えはもちろん no である．さらに，わずかな違いを起す遺伝要因の検出には膨大な数の検体数を要する．もちろん，そのような遺伝要因を膨大なコストをかけて検出する意義についても疑問であろう．Common disease の原因は common variant であると，Eric Lander らにより提唱された，いわゆる common disease－common variant（CD－CV）hypothesis である[3]．ありふれた病気の原因は頻度の高い多型による（common variant），またその多型は共通の祖先から生じている（common variant）という考えである．一方，common disease－rare variant も存在する．実際に血中 HDL コレステロール値を遺伝的に規定している遺伝子多型は，頻度が低いが効果の強いことが示されている[4]．Rare allele はチップ上に搭載されていないので，そもそ

表1　ゲノム全域アソシエーション・スタディ（GWAS）による疾患遺伝子解析

疾患	検体数	結果 SNP 遺伝子	有意差	Odds ratio	SNP Number	Publication Year	Author	Journal
2 型糖尿病	1,464 cases, 1,467 controls	rs10811661 *CDKN2A/ CDKN2B*	5.4×10^{-15}	1.2	500k SNPs	2007	Broad Institute	Science 316, 1331−1336
		rs20769013 *CDKAL1*	4.1×10^{-11}	1.12				
		rs7903146 *TCF7L2*	1.0×10^{-48}	1.37				
		rs780094 *GCKR*	3.7×10^{-8}					
	1,924 cases, 2,938 controls 3,757 cases, 5,346 controls	replicated			500k SNPs	2007	Zeggini et al.	Science 316, 1336−1341
	1,161 cases, 1,174 controls	replicated			315k SNPs	2007	Scott et al.	Science, 316, 1341−1345
2 型糖尿病	1,363 cases, 1,353 controls 2,617 cases, 2,894 controls	rs7903146 *TCF7L2*	1.5×10^{-34}	1.65	393k SNPs	2007	Sladek et al.	Nature 445, 881−885
		rs1326634 *SLC30A8*	6.1×10^{-8}	1.53				
2 型糖尿病	1,399 cases, 5,275 controls	rs7903146 *TCF7L2*	1.8×10^{-10}	1.38	300k SNPs	2007	Steinthorsdottir et al.	Nat Genet 39, 770−775
		rs7756992 *CDKAL1*	7.7×10^{-9}	1.2				
肥満	38,759 perticipants	rs9939609 *FTO*	3×10^{-35}	1.67	400k SNPs	2007	Frayling et al.	Science 316, 889−894
冠動脈疾患	322+311 cases, 312+326 controls 23,000 participants	rs10757274 *CDKN2A/ CDKN2B*	1.2×10^{-20}	1.28	100k SNPs	2007	McPherson et al.	Science 316, 1488−1491
	4,587 cases, 12,767 controls				300k SNPs	2007	Helgadottir	Science, 316, 1491−1493
クローン病	567+547 cases, 571+548 controls	rs2066843 *CARD15*	2.86×10^{-9}		308k SNPs	2006	Duerr et al.	Science 314, 1461−1463
		rs11209026 *IL23R*	5.05×10^{-9}					
クローン病	735 cases, 368 controls	rs2241880 *ATG16L1*	4.0×10^{-8}		200k SNPs	2007	Hampe et al.	Nat Genet 39, 207−211

疾患	検体数	結果 SNP 遺伝子	有意差	Odds ratio	SNP Number	Publication Year	Author	Journal
クローン病	988 cases, 1,007 controls	rs2241880 *ATG16L1*	6.4×10^{-8}		318k SNPs	2007	Rioux et al.	Nat Genet 39, 596−604
		rs224136 *ZNF365*	7.9×10^{-6}					
乳癌	4,398 cases, 4,316 controls 21,860 cases, 22,578 controls（2nd stage）	rs2981582 *FGFR2*	2×10^{-76}	1.63	228k SNPs	2007	Easton et al.	Nature 447, 1087−1093
乳癌	1,600 cases, 11,563 controls 4,554 cases, 17,577 controls	rs13387042	1.3×10^{-13}	1.2	300k SNPs	2007	Stacey et al.	Nat Genet 39, 865−869
		rs3803662	5.9×10^{-19}	1.28				
乳癌	1,145 cases, 1,142 controls 1,776 cases, 2,072 controls	rs1219648 *FGFR2*	1.1×10^{-10}	1.64	528k SNPs	2007	Hunter et al.	Nat Genet 39, 870−874
前立腺癌	1,453 cases, 3,064 controls	rs1447295	6.4×10^{-18}	1.53	300k SNPs	2007	Gudmundsson et al.	Nat Genet 39, 631−637
	1,172 cases, 1,157 controls	rs6983267	9.42×10^{-13}	1.26	550k SNPs	2007	Yeager et al.	Nat Genet 39, 645−649
躁うつ病	2,000 cases, 3,000 controls	rs420259 *OALB2/ NDUFAB1*	6×10^{-8}	2.08	500k SNPs	2007	The Wellcome Trust Case Control Consortium	Nature, 447, 661−678
冠動脈疾患	2,000 cases, 3,000 controls	rs1333049 *CDKN2A/ CDKN2B*	1.8×10^{-14}	1.9	500k SNPs	2007	The Wellcome Trust Case Control Consortium	Nature, 447, 661−678
クローン病	2,000 cases, 3,000 controls	rs11805303 *IL23R*	6.45×10^{-13}	1.86	500k SNPs	2007	The Wellcome Trust Case Control Consortium	Nature, 447, 661−678
		rs10210302 *ATG16L1*	7.1×10^{-14}	1.85		2007	The Wellcome Trust Case Control Consortium	Nature, 447, 661−678
関節リウマチ	2,000 cases, 3,000 controls	rs6679677 *PTPN22*	4.9×10^{-26}	3.32	500k SNPs	2007	The Wellcome Trust Case Control Consortium	Nature, 447, 661−678
1型糖尿病	2,000 cases, 3,000 controls	rs6679677	1.1×10^{-26}	5.19	500k SNPs	2007	The Wellcome Trust Case Control Consortium	Nature, 447, 661−678
		rs17696736 *ten genes*	2.17×10^{-15}	1.94		2007	The Wellcome Trust Case Control Consortium	Nature, 447, 661−678
2型糖尿病	2,000 cases, 3,000 controls	rs4506565 *TCF7L2*	5.7×10^{-13}	1.36	500k SNPs	2007	The Wellcome Trust Case Control Consortium	Nature, 447, 661−678